

A. ŚWIĄTONIOWSKI\*, J. SIŃCZAK\*\*, A. ŁUKASZEK-SOŁEK\*\*, J. SCHMIDT\*\*\*

## ANALYSIS OF FORGING PROCESS OF THE NiCrN SUPERALLOY FOR MOTOR BOAT DRIVING SHAFT

## ANALIZA PROCESU KUCIA SUPERSTOPU NiCrN NA WAŁY NAPĘDOWE ŚRUBY JEDNOSTKI MORSKIEJ

Superalloys containing nickel and chromium display high deformation resistance and low plasticity during high-rate plastic forming processes, thus limiting the potentials to improve their mechanical parameters. At the aim to overcome this problem an NiCrN superalloy has been found. In this paper the analysis of forging of this NiCrN superalloy has been presented. Mathematical FEM model of the process are verified by experimental tests run on a double-acting power hammer. Tests reveal, that plastic working of the NiCrN alloy combined with thermal treatment improves its strength by nearly 25%, at the same time its plastic deformability remains the same. Research work has revealed very high resistance to corrosion of the alloy when subjected to stress and marine environment.

*Keywords:* NiCrN superalloy, Closed-die forging process

Superstopy opracowane na bazie niklu i chromu charakteryzują się dużym oporem odkształcenia i niską zdolnością do odkształceń plastycznych. Ogranicza to w poważnym stopniu możliwość podniesienia ich własności mechanicznych na drodze przeróbki plastycznej, a tym samym i zakres ich zastosowania jako materiału konstrukcyjnego. W celu rozwiązania tego problemu został opracowany nowy, unikalny skład chemiczny stopu NiCrN. Przeprowadzono modelowanie numeryczne procesu kucia matrycowego opracowanego stopu oraz weryfikację eksperymentalną na młocie parowo-powietrznym podwójnego działania. Przeprowadzone badania pozwoliły stwierdzić, że w wyniku odkształcenia plastycznego stopu NiCrN połączonego z obróbką cieplną można uzyskać blisko 25% wzrost jego własności wytrzymałościowych. Ponadto wykazano bardzo wysoką odporność na korozję stopu.

### 1. Introduction

Elements of hydraulic machines (water turbines, pumps), screw propellers (Fig.1) and cables of various cross-section are subject to damage due to cavitation processes [1-4].

Among well-known construction materials, alloys containing nickel and chromium are most resistant to this form of corrosion [5, 6].

However, those alloys display high deformation resistance and low plasticity during high-rate forming processes, thus limiting the potentials to improve their mechanical parameters and to shape their structure, adapting it to the service loads.

An attempt to overcome this difficulty was made by collaborating researchers and foundry engineering experts, who developed an NiCrN alloy, containing chromium, endogenous modified nitrogen and elements forming

nitrides [7, 8]. This alloy was obtained experimentally in Foundry Plant in Cracow.

### 2. Characteristics of NiCrN superalloy

The chemical composition of the alloy (45% chromium, 45% nickel and nitrogen contents approaching 0.47%) is established on the basis of forecasting methods and it is found to be optimal in the context of improving its mechanical properties by way of plastic treatment.

This alloy consists of nickel austenite (phase  $\gamma$ ) as the matrix, crystallised in the shape of dendrites.

In the interdendritic space is the  $\gamma$ - $\alpha$  eutectic in the amount of 5-10% and the phase  $\gamma'$  in the form of compound with the general formula given as  $Ni_3(Al, Ti, Cr)$ . The matrix features also the precipitates of titanium carbonitrides of small geometry and oxide contaminants.

\* AGH UNIVERSITY OF SCIENCE AND TECHNOLOGY, DEPARTMENT OF MANUFACTURING SYSTEMS, 30-059 KRAKÓW, 30 MICKIEWICZA AV., POLAND

\*\* AGH UNIVERSITY OF SCIENCE AND TECHNOLOGY, DEPARTMENT OF METAL FORMING, 30-059 KRAKÓW, 30 MICKIEWICZA AV., POLAND

\*\*\* CRACOW UNIVERSITY OF TECHNOLOGY, FACULTY OF MECHANICAL ENGINEERING, 31-155 KRAKÓW, 24 WARSZAWSKA STR., POLAND

In order to ensure the required parameters of the melting process, the amount of the brittle phase should not exceed 5%, including the phase  $\eta$ , TCP phases  $\sigma$  and  $\mu$ , the Laves's phase as well as intermetallic compounds of nickel, aluminium, titanium, chromium.

Tensile strength of the cast alloy is:  $R_m = 597$  MPa and may be increased in the course of thermal treatment at 1050°C to:  $R_m = 768$  MPa.

### 3. Model testing of the forging process of NiCrN

#### Open die forging in flat and shaped dice

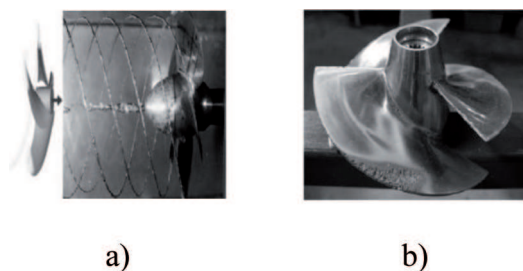


Fig. 1. Screw propeller damage caused by cavitation process

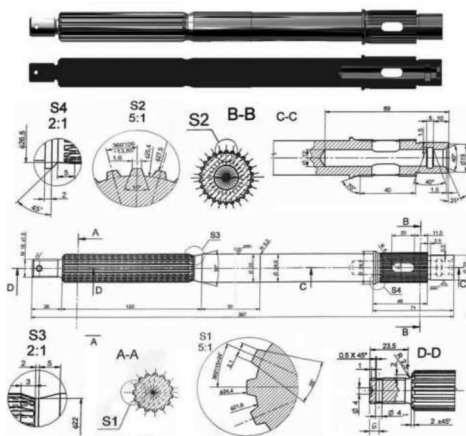


Fig. 2. Driving shaft  $\varnothing 335$  of the motor boat screw propeller (Type OP-1960-00-04/1)

Model tests, performed to find out how plastic treatment should improve the strength parameters of the NiCrN alloy, involve the forging process of the driving shaft in a screw propeller for motor boat.

The shaft is a good representative of a structural component subjected to a complex state of dynamic stresses and operated in strongly corrosive environment, hence such stringent requirements that the material it is made of has to meet. Besides, because of these strength requirements, the ship-building sector shows a major interest in such alloys and their potential applications.

In the most general case, the process of shaft forging might be considered as a series of subsequent swelling and elongation operations.

During the first series of tests, the NiCrN ingots 40 mm in diameter were subjected to free swelling in flat and shaped dice on a double-acting power hammer (Figure 3).



Fig. 3. Sample of the NiCrN ingot after free swelling in flat dice

This process does not require specialist equipment, is relatively cheap and hence it seems most adequate when performing preliminary tests or producing single units or in small-scale manufacturing (up to 20 items per year).

The results reveal that the potentials of alloy shaping by plastic treatment are rather limited.

The correct process of material flow is observed only with reference to the lowest values of the relative strain, for process temperatures both in the lower and upper range. At higher degrees of forging,  $\varepsilon = 3.0-4.0$  which were applied in order to obtain fine-grained, plastically deformable crystalline structure of the material to improve its mechanical properties, cracks could be observed on side surfaces in the majority of forged specimens. The number of cracks tends to increase with the degree of deformation, until cracks will appear on the front surfaces, too.

This effect may be attributable to the complex and strongly non-uniform state of stress, from triaxial compression to two-axial tension, generated in the forged section in the consequence of the application of external forces.

This state corresponds to the state of strain whereas the factors enhancing the non-uniformity of strain will also enhance the contribution of tensile stress near the side surface of the metal, at the same time leading to increased compression inside the forged section. The factors reducing this non-uniformity have the reverse effect.

As the NiCrN alloy displays a strong tendency to cracking, well demonstrated during the free elongation processes in flat and shaped dice, the researchers decided that further attempts at forging a shaft shall be made in a maximally closed die impression, to achieve the state of triaxial compression stress.

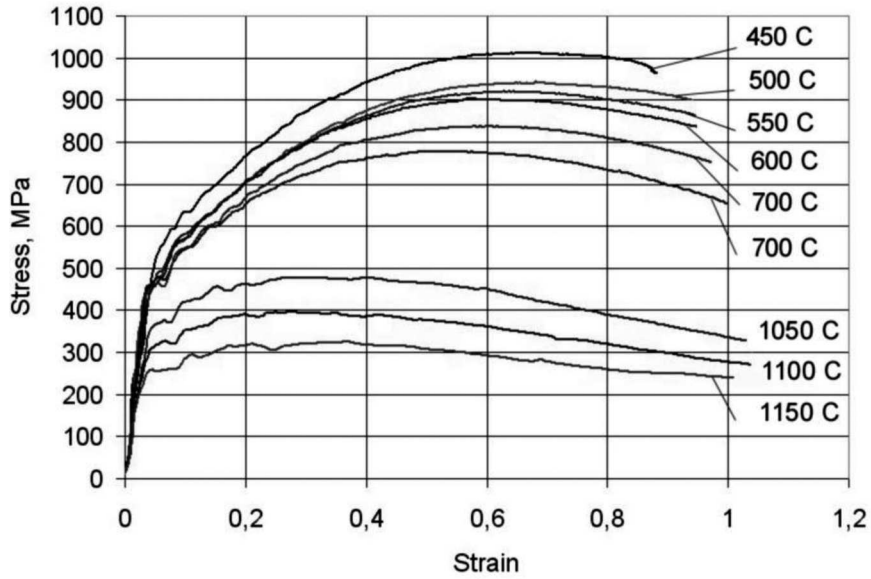


Fig. 4. Strain-stress characteristics of the alloy NiCrN in the function of grown down temperature at the deformation rate  $40 \text{ s}^{-1}$

### Single-impression dice

In accordance with the conventional methodology, tests were preceded by a thorough mathematical analysis of the modeled process supported by a commercially available FEM software –QForm3D and using the NiCrN characteristics obtained on the Gleeble 3800 simulator [9].

Underlying distributions of strain and strain indicators and the temperature distribution are governed by the thermo-mechanical model of the strain process. The calculation procedure assumes the elastic-viscous-plastic model of a body being deformed and the Levanov’s friction model, given by the formula:

$$\tau = m \frac{\sigma_p}{\sqrt{3}} \left( 1 - e^{-1.25(\sigma_n/\sigma_p)} \right) \quad (1)$$

where:  $\sigma_n$  – normal stress

$\sigma_p$  – flow stress

$m$  – friction factor.

The assumed model does not take into account the cracking criterion throughout the entire free flow regime, where the state of stress proves most unfavourable (due to the occurrence of tensile stresses), whilst the material being deformed retains its cohesion.

The material flow curve is the function of temperature, strain and deformation rate. Accordingly, we get

$$\sigma_H = \sigma_p = f \left( \varepsilon_i \frac{d\varepsilon_i}{dt}, T \right) \quad (2)$$

In order to determine the kinematics of metal flow during a real process of shaft forging in a power hammer, the subsequent FEM simulations assume the boundary

conditions specific to the process: the charge 35 mm and 40 mm in diameter, 370 in length, heating temperature  $1150^\circ\text{C}$  [10], ingot transport time from the furnace to the power hammer equals 7s, die temperature  $300^\circ\text{C}$ .

The value of the friction factor is taken as 0.4 for the applied lubricant gw-st-h.

Simulations were performed for two deformation rates: the constant rate equal to  $50 \text{ s}^{-1}$  and the variable one, associated with the power hammer characteristics, the initial pressing rate being 6 m/s.

Assuming the feed material to the forging process to be an ingot with the original cast structure, the numerical procedure is aimed to find the distribution of strain intensity  $\varepsilon_i$ , in order to determine the degree of forging  $k$  depending on the die geometry and the applied forging technology.

$$k = e^{\varepsilon_i} \quad (3)$$

The calculation procedure uses thirty records, each involving five steps. The FEM grid in the last record consists of 68 390 elements.

Representative examples of thus performed simulations of the mathematical model of shaft forging during the subsequent hammering operations include the thermal state, strain intensity and the average stress pattern).

It has been shown that variations of the hammering rate are accompanied by changes of the material flow kinematics and prolonging of the deformation time leads to the temperature decrease during the final stage of forging. The thermal states of the forging obtained for two charge diameters are comparable.

An evaluation of the strain distribution reveals that during the elongation process the state of strain proves to be non-uniform over the entire range of investigated

parameters. The strain distribution pattern reveals several characteristic deformation zones, which strongly impact on the degree of forging and properties of the forged material.

It is readily apparent that single-process forging induce relatively small plastic working, that applies mostly to the regions of deepest die impression under its upper and lower surface, due to minor displacements of the material. In the consequence, with minor working of the forging structure, we should expect only limited improvements of mechanical and plastic properties of the finished products.

A major gradient of strain intensity in the flash region is a natural phenomenon during the final stage of forging in a half die. In order to reduce the non-uniformity of deformations, it is required that that the flashing be minimized in the finishing impression, which may lead, however, to the reduction of the degree of forging in the forging volume.

It is readily apparent (Figure 5 and 6) that the process of single forging in an open die does not generate tensile stresses, which is a major advantage in the case of materials, such as NiCrN, which tend to crack during the plastic treatment. Compressive stresses, on the other hand, are considerable, in excess of 2000 MPa.

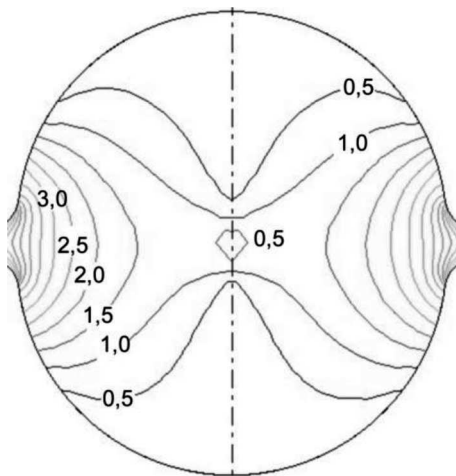


Fig. 5. Deformation intensity in the forged shaft cross-section during the hammer forging; the charge diameter being  $\Theta = 40$  mm

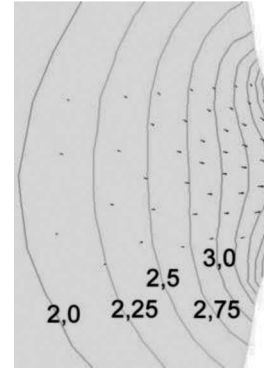


Fig. 6. High degree of forging zone in the shaft forged from the charge  $\Theta = 40$  mm in diameter

Non-uniformity of the triaxial state of stress in the forging and flash zone is also revealed in the deformation pattern of the square grid system in Figure 7.



Fig. 7. 3D distribution of the grid in the model of a shaft forging (the charge diameter being 40 mm)

These results of mathematical modeling of the forging process were confirmed experimentally.

The NiCrN ingots 40 mm in diameter and 370 in length are subjected to single-impession die forging by six hammering actions. Thus obtained forging is shown in Figure 8.

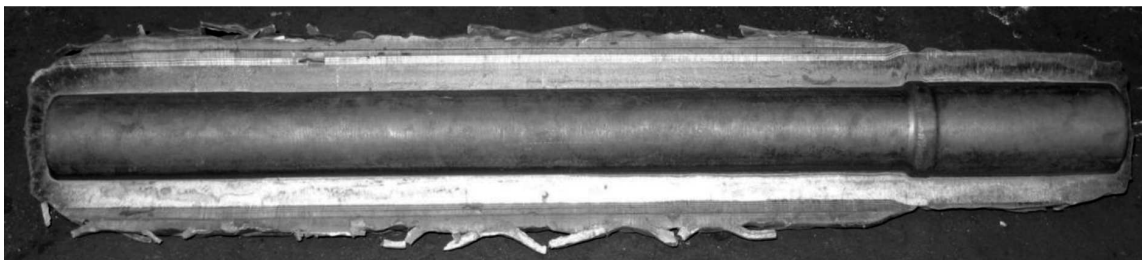


Fig. 8. Shaft forging with a flash (after cooling to the room temperature)

#### 4. Testing the properties of the alloy NiCrN after die forging

Tests were run on specimens made from forgings without any thermal treatment. After the deformation process they were homogenized at 1050°C and solution heat treated for 60 minute.

Specimens were collected both from the cylindrical part of the forging and from the flash section because of major variations in their degree of forging, associated with strain intensity  $k$ .

Microstructure of specimens collected from the NiCrN forgings is shown in Figure 9 and Figure 10.

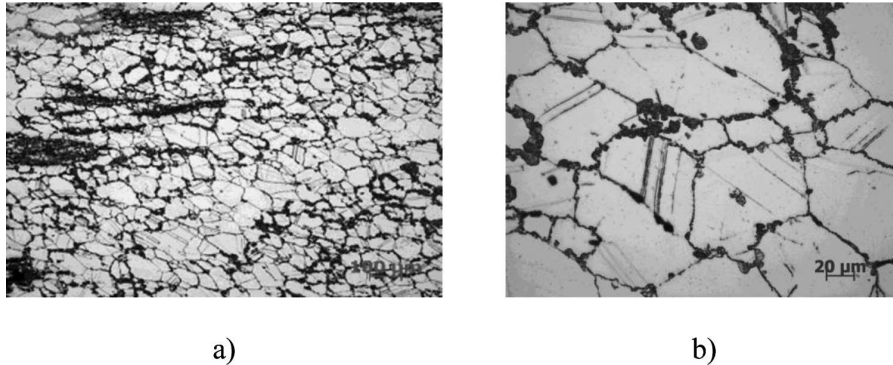


Fig. 9. Microstructure of the alloy NiCrN obtained after the forgings (a-zoom 100 x, b-zoom 500 x)

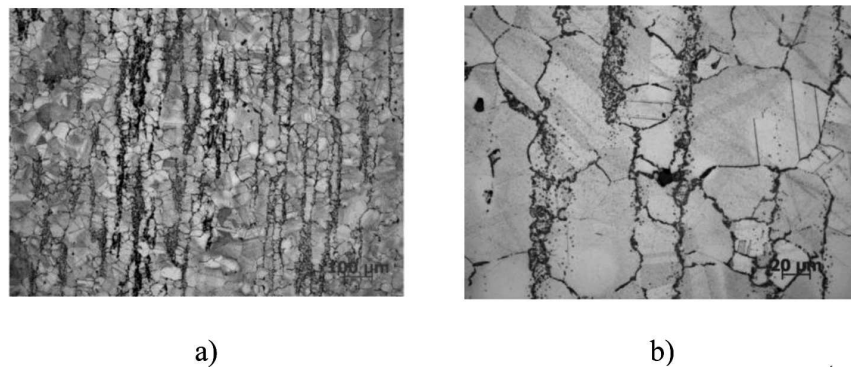


Fig. 10. Microstructure of the alloy NiCrN obtained after the forgings and a subsequent thermal treatment process (a-zoom 100 x, b-zoom 500 x)

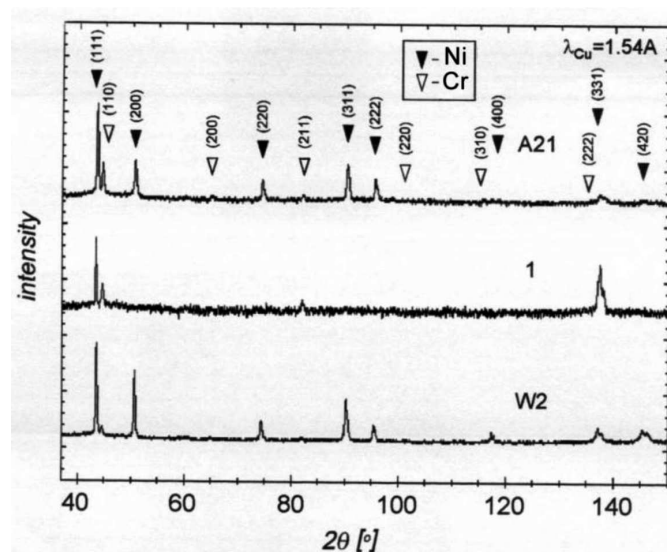


Fig. 11. X-ray diagrams of the alloy NiCrN, cast and forging (after heat-treated)

We can easily observe the grain geometry of austenite phase  $\gamma$  of various orientation, with twinned crystals which appeared there as a result of thermal treatment. These observations are corroborated by experimental data, obtained by the X-ray diffraction method.

Structure of the alloy NiCrN clearly reveals major variations in the crystalline texture with respect to the microsection while the most significant differences are registered for cast samples. All specimens contain the two major phases: i.e. the solid solution Ni(Cr) and Cr(Ni), as well as tiny amounts of unidentified phase (maybe an ordered one). The alloy matrix is the phase Ni(Cr)- a solid solution with the FCC lattice of chromium in nickel, the other phase Cr(Ni) being a solid solution of nickel in chromium, with the BCC lattice. The microstructure of the alloy contains the phase Ni<sub>2</sub>Cr and phases containing nitrogen, such as compounds: Cr<sub>2</sub>N,  $\epsilon$ ,  $\pi$ .

The forging process made the grains finer, the smallest grain in the solid solution Ni(Cr) is found in the sample after forging and heat treatment. Lattice parameters reveal considerable amounts of Cr and relatively smaller contents of Ni in the Cr lattice.

Changes of the NiCrN structure are accompanied by changes of the alloy's mechanical properties, which is illustrated in Table 1.

TABLE 1

Comparison of mechanical properties of the alloy NiCrN in the cast condition and after plastic deformation and thermal treatment. (samples collected from the cylindrical section of the shaft forging 40 mm in diameter)

Condition of the material	Tensile strength MPa	Offset yield strength MPa	Elongation A %	Brinell hardness HBW
Casting with heat treatment	768	612	33	229
Forging with heat treatment	972	694	52	196

Tabulated data reveal a 25% increase of strength parameters of the alloy NiCrN after plastic deformation and thermal treatment. Of particular importance is its behaviour and extended range of the elastic-plastic deformation regime.

## 5. Final conclusions

1. Tests reveal that mechanical properties of the alloy NiCrN might be largely modified by applying plastic working technology combine with heat treatment. Hence it is possible to use this alloy to manufacture high-quality machine components working in highly corrosive envi-

ronment and capable of handling dynamically variable working loads of large amplitudes.

2. As the potentials of plastic treatment of the alloy NiCrN are limited, in order to achieve the high degree of forging and restructure the entire cross-section of the forging, it is required that the triaxial state of stress should be generated within the forging. This state corresponds to the multi-process die forging.

3. A good correspondence between theoretical data and experimental results confirms the adequacy of the assumptions underlying the mathematical model of the process, supported by the FEM approach, and hence its usefulness in selection of the optimal process technology.

4. Research data indicate that the mechanism of deformation remains a major determinant of resistance to deformation during the plastic working of the alloy NiCrN. For the given alloy composition and temperature, this mechanism depends chiefly on process temperature, the degree of deformation and the deformation rate.

Sensitivity of the alloy NiCrN to the conditions of thermal treatment is another major issue and the deformation rate has to be precisely controlled so that its too low value should not lead to the significant decrease of the metal temperature, and when it is too high, the metal might become overheated, which leads to non-uniformity of grains in the forging volume, which is responsible for anisotropy of its strength parameters.

The temperature of heating the alloy NiCrN for forging should not be lower than 1150°C. At that temperature the alloy displays an adequate plasticity to meet the requirements of the process, guaranteeing the forgings with the specified shape and dimensions. Besides, forging temperature impacts on the structure of the half-finished products and the value and stability of its strength parameters and plastic properties.

## Acknowledgements

Financial support for this research programme was provided by the Polish Ministry of Science and Higher Education (Project No: R 15 039 02).

## REFERENCES

- [1] J.W. Brooks, Forging of superalloys; *Materials and Design* **21**, 297-303 (2000).
- [2] B.P. Bewlay, M.F.X. Gigliotti, C.U. Hardwicke, O.A. Kaibyshev, F.Z. Utyashev, G.A. Salishev, Net shape manufacturing of aircraft engine disks by roll forming and hot die forming; *Journal of Materials Processing Technology* **135** (2-3 SPEC), 324-329 (2003).

- [3] Y.-S. Na, J.-T. Yeom, N.-K. Park, J.-Y. Lee, Simulation of microstructures for Alloy 718 blade forming using 3D FEM simulator; *Journal of Materials Processing Technology* **141** (3), 337-342 (2003).
- [4] S. Tin, P.D. Lee, A. Kermanpur, M. Rist, M. McLean, Integrated modeling for the manufacture of Ni-based superalloy discs from solidification to final treatment; *Metallurgical and Materials Transactions A: Physical Metallurgy and Materials Science* **36** (9), 2493-2504 (2005).
- [5] P.W. Schilke, R.C. Schwant, *The Minerals, Metals & Materials Society* 25-34 (2001).
- [6] T. Shibata, T. Takahashi, J. Taira, T. Kure, *The Minerals, Metals & Materials Society* 161-172 (2001).
- [7] A. Kazakov, J. Schmidt, Developing and experimental verification of the technology for producing dispersion reinforced cast nickel-chromium alloys. *Proceeding of the Cast Composites Conference, Zakopane (Poland)*, 172-178, (18-20 October 1995).
- [8] J. Schmidt, A. Kazakov, Investigation of CrNiN alloys properties as a material for propeller casting used by shipbuilding industry. *Proc. of 1<sup>st</sup> Int. Conf. on Advanced Materials Processing, Rotorua, New Zealand*, 633-637, (19-23 November 2000).
- [9] J. Sińczak, A. Świątoniowski, J. Schmidt, J. Szostak, *Rudy i Metale Nieżelazne* **53-7**, 418-424 (2008).
- [10] D. Cai, L. Xiong, W. Liu, G. Sun, M. Yao, Characterization of hot deformation behavior of Ni-base superalloy using processing map; *Materials and Design* **30**, 921-925 (2009).